Proceedings of the 12th International Conference on Fluid Flow, Heat and Mass Transfer (FFHMT 2025)
July 15, 2025 - July 17, 2025 | Imperial College London Conference, London, United Kingdom
Paper No. 240
DOI: 10.11159/ffhmt25.240

Velocity and Turbulent Kinetic Energy Prediction with Darcy-Forchheimer Model for Water Intakes

Cumhur Ozbey[1], Serhat Kucukali[2]
[1]Hacettepe University, Civil Engineering Department, Hydraulics Division,
Ankara, Turkey
cumhurozbey@hacettepe.edu.tr; kucukali78@gmail.com

Abstract **-** The flow field and turbulent characteristics in the vicinity of water intakes are numerically modeled by using the Darcy-Forchheimer porous media approach coupled with LES. Two types of barriers used at hydropower plants were analyzed, namely the rectangular and Oppermann profiles, having clear bar spacing of b=20 mm and b=10 mm, respectively. For both profiles, simulations were run under two different angles of α=30° and α=45°. The comparison between the experimental and CFD results revealed acceptable error ranges (<10%) for both velocity and turbulent kinetic energy, yielding reliable prediction accuracies of the Darcy-Forchheimer model. Also, treating the water intakes as a porous medium led to a significant reduction in the computational cost and time.

Keywords**:** Water Intake, CFD Modeling, Darcy-Forchheimer Model, LES, Flow Field, Turbulent Kinetic Energy.

1. Introduction

Hydropower plants (HPPs) can block or delay the passage of downstream migrating fish, leading to a reduction in fish populations worldwide. Particularly, run-of-river type HPPs present a significant risk to downstream migration, leading to delays, injuries, and fatalities during turbine passage [1,2]. Accordingly, to protect fish species as well as to prevent the passage of debris and driftwood toward the hydro-machinery, either conventional trash racks having rectangular bars or hydro-dynamically designed bar profiles are applied at the water intake structures of downstream passage facilities.

Within the scope of this study, a specific type of physical barrier, the streamlined Oppermann fine screen, is numerically investigated. Head losses are reduced through improved hydraulic conditions around this Oppermann screen, which is implemented in various small and medium-scale hydropower facilities [3]. These screens are characterized by several key advantages, including effective fish protection achieved through narrow bar spacing, a rounded leading edge, and a smooth bar surface, as well as a hydraulically optimized design, enhanced hydropower efficiency, reduced overall weight, and efficient cleaning and manufacturing [4]. The numerically modeled 3D solid profile of the screen and the corresponding bar details are shown in Figure 1. As illustrated, the thickness of the leading and trailing edges are 6 mm and 1.5 mm, respectively, providing a streamlined bar shape. Also, the clear bar spacing is 10 mm, making it a fine screen, and the total bar depth is 83 mm.

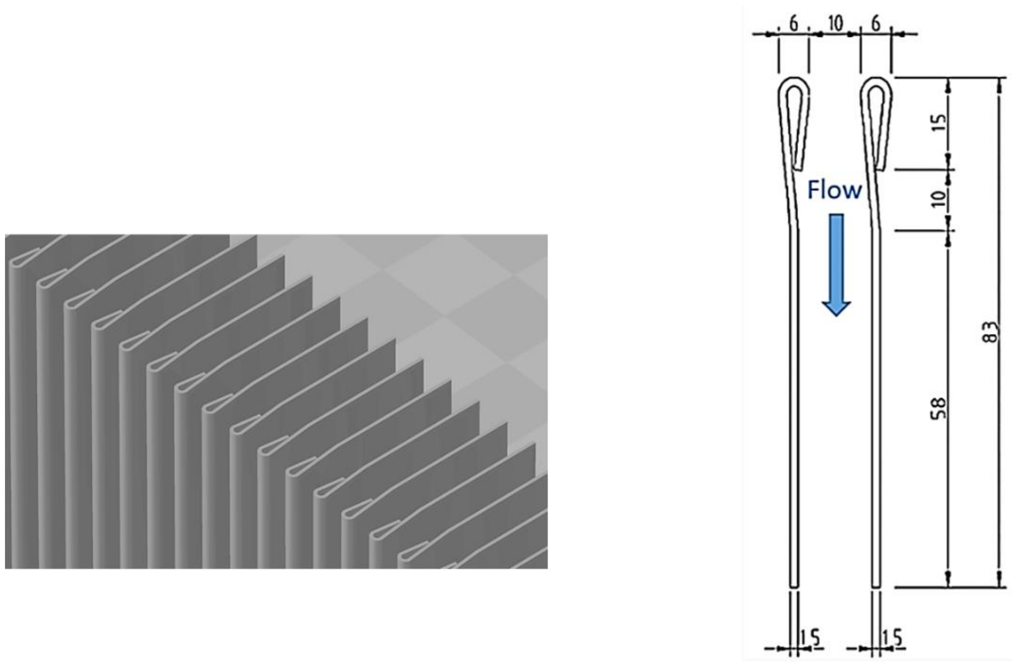

(a) (b)

Fig. 1: (a) 3D solid model of the Oppermann profile, (b) bar details in mm.

The water intakes that are used at HPPs should be installed horizontally angled to the streamwise flow direction in order to provide a barrier effect leading to optimal fish guidance [5]. In recent years, the flow fields around the angled racks have been extensively investigated through various experimental studies [6,7,8,9,10], where both rectangular and hydrodynamic bar profiles were tested under different rack angles. Contrarily, CFD studies focusing on the flow fields in the vicinity of angled water intakes have been relatively limited in the existing literature. For instance, the studies by [11] and [12] involved numerical investigations of angled racks with various bar profiles, performed under different turbulence models. However, in these CFD studies, the angled racks were modeled using the actual bar geometries, resulting in a substantial total cell count within the solution domain. This is primarily due to the requirement for finer mesh resolutions near the rack structure. To address this numerical limitation, the present study employs a porous media approach using the Darcy-Forchheimer model to simulate the flow through angled water intakes, thereby aiming to reduce the computational cost and time. Thus, the flow fields and turbulent quantities around the water intake structures are investigated, and the corresponding prediction accuracy and applicability of the Darcy-Forchheimer model are tested.

2. Experimental Reference Case for CFD Validation

The CFD validation for the Darcy-Forchheimer model was conducted using the experimental data provided by [13], in which both a conventional rectangular trash rack and the Oppermann fine screen were tested in a 2-m wide and 30-m long recirculating laboratory flume. Accordingly, a constant flow depth of 0.6 m and a discharge value of 225 L/s were maintained in the system, resulting in an approach Froude number of 0.206 for all cases. Throughout the experiments, the clear bar spacing of b=10 mm and b=20 mm was used for the Oppermann and rectangular bar profiles, respectively. Two different horizontal angles, α=30°, and α=45° were tested for both profiles. The overall parameters for the experimental study of [13] for both rectangular and Oppermann profiles are summarized in Table 1, where identical hydraulic conditions are simulated in this present study.

Table 1. Summary of the experimental conditions of [13] used in the CFD model.

Water Intake Type	Q (L/s)	V (m/s)	y_1 (m)	y_2 (m)	B (m)	b (mm)	α (-)	Fr_1 (-)
Oppermann	225	0.5	0.6	0.6	2	10	30°, 45°	0.206
Rectangular	225	0.5	0.6	0.6	2	20	30°, 45°	0.206

* Q = discharge, V = approach flow velocity, y_1 = upstream flow depth, y_2 = downstream flow depth, B = channel width, b = clear bar spacing, α = angle of the water intake, and Fr_1 = approach Froude number.

The instantaneous local velocities in all directions were measured at 60 and 90 different points for the rectangular and the Oppermann profiles, respectively. The measurement data were collected by a 10 Hz Acoustic Doppler Velocimetry (ADV) probe with a sampling duration of 30 seconds, with an accuracy of ±1%.

From the 3D ADV measurements, the resultant velocity, V_{res}, can be calculated from:

$$V_{res} = \sqrt{u^2 + v^2 + w^2} \tag{1}$$

where u, v, and w refer to the velocity components in x, y, and z directions, respectively. The turbulent kinetic energy is used as an indicator of the turbulence level, which is defined as:

$$k = \frac{1}{2}\left(\overline{u'^2} + \overline{v'^2} + \overline{w'^2}\right) \tag{2}$$

where k is the turbulent kinetic energy per unit mass, and u', v', and w' are the fluctuating velocity components in the streamwise, spanwise, and vertical directions, respectively.

3. CFD Modeling

The numerical modeling was performed in FLOW-3D, which is a commercially available computational fluid dynamics (CFD) software that employs the finite volume method (FVM) throughout the simulations [14]. Accordingly, the flow through the rectangular trash rack and the Oppermann fine screen was numerically modeled with a porous media approach rather than running simulations based on the actual bar geometries. The corresponding numerical results were then compared with the experimental data of [13] in accordance with the flow fields and turbulent quantities.

For the treatment of turbulence, the Large Eddy Simulation (LES) turbulence model was applied in the CFD models where the large-scale structures in the computational domain are resolved directly [15], and the sub-grid scale structures are modeled [16]:

$$\tau_{\mathrm{ij}} = -2v_t\bar{\mathrm{S}}_{ij} \tag{3}$$

$$\bar{\mathrm{S}}_{ij} = \frac{1}{2}\left(\frac{\partial\bar{\mathrm{u}}_i}{\partial x_j} + \frac{\partial\bar{\mathrm{u}}_j}{\partial x_i}\right) \tag{4}$$

where τ_{ij} is the anisotropic stress tensor, $\bar{S}_{ij}$ refers to the resolved rate of strain, v_t denotes the turbulent viscosity, $\bar{u}_i$ is the resolved velocity field, and x shows the Cartesian direction.

3.1. Darcy-Forchheimer Model

According to the Darcy-Forchheimer porous media model, the pressure drop due to a porous region can be defined by the following semi-empirical relation:

$$-\nabla p = A|u_D|\mu\frac{(1-\phi)^2}{\phi^3} + \mathrm{B}|u_D|^2\rho\frac{(1-\phi)}{\phi^3} \tag{5}$$

where ∇p refers to the pressure drop, A and B denote the Forchheimer drag coefficients, u_D represents the Darcian velocity, μ is the dynamic viscosity, ρ is the fluid density, and ϕ is the porosity. Typically, depending on the type of porous medium, the drag coefficients A and B are determined experimentally [17]. Considering the experimental data of [13], corresponding Forchheimer drag coefficients for rectangular and Oppermann profiles have been calculated from Eqn. (5). Table 2 summarizes the drag coefficients as well as the porosity values for α=30° and α=45° cases that are applied in the numerical model.

Table 2. Forchheimer drag coefficients and porosity values used in the CFD model of [13].

Screen Profile	Drag Coefficient A (1/m)		Drag Coefficient, B (-)		Porosity, ϕ (-)	
	$\alpha = 30°$	$\alpha = 45°$	$\alpha = 30°$	$\alpha = 45°$	$\alpha = 30°$	$\alpha = 45°$
Oppermann	-52796.8	-56203.1	0.251	0.269	0.625	0.625
Rectangular	-57906.2	-59609.3	0.298	0.307	0.796	0.796

* α = angle of the water intake.

3.2. Model Setup and Meshing

Figure 2 shows the three-dimensional CFD model of the experimental setup by [13], where the x, y, and z axes denote the spanwise, streamwise, and vertical directions, respectively. Accordingly, the porous region is oriented at a 30° angle relative to the main flow direction, representing the water intake structures. Corresponding instantaneous 3D velocities were numerically measured at probe points located 0.1 m upstream and 0.2 m downstream of the porous medium. As an initial condition, a flow depth of 0.6 m was defined in the entire solution domain, which is coupled with a velocity boundary condition at the inlet. For the sidewalls and the channel bottom, the symmetry and wall boundary conditions were applied, respectively. At the outlet, the pressure boundary condition was employed along with a given flow depth of 0.6 m., and the atmospheric pressure was satisfied at the free surface. Lastly, the initial time step was defined as 0.001 seconds, and the following time steps were dynamically computed by the software based on the stability criterion.

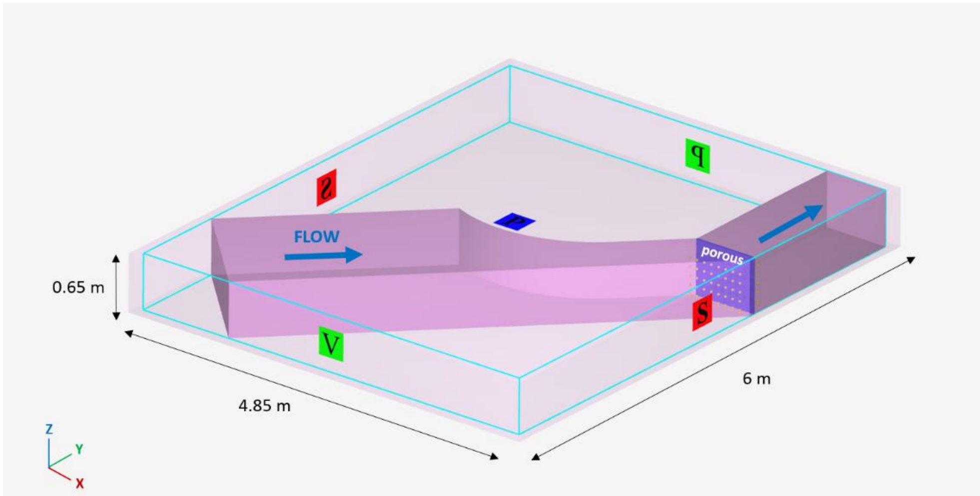

Fig. 2: Three-dimensional CFD model for 30° angled case showing the porous medium (blue), measurement points (yellow), and boundary conditions where V = velocity, P = specified pressure, and S = symmetry. The dimensions of the solution domain are given.

A mesh sensitivity analysis was performed considering both resultant velocity and turbulent kinetic energy errors between the experimental data of [13] and the CFD results for the Oppermann fine screen (Table 3). It can be seen that, for both tested angles, the relative errors of V_{res} and k parameters remain almost the same after the mesh size of 0.02 meters, resulting in a mesh-independent solution.

Table 3. Mesh sensitivity analysis based on the mean absolute percentage error (MAPE) values at 90 data points for the Oppermann fine screen with bar spacing of b=10 mm.

Mesh size (m)	$\alpha = 30°$		$\alpha = 45°$	
	V_{res} (m/s)	k (m^2/s^2)	V_{res} (m/s)	k (m^2/s^2)
0.05	MAPE=7.8 %	MAPE=13.8 %	MAPE=10.8 %	MAPE=15.0 %
0.04	MAPE=7.2 %	MAPE=10.8 %	MAPE=10.5 %	MAPE=11.6 %
0.03	MAPE=5.3 %	MAPE=8.4 %	MAPE=9.3 %	MAPE=8.5 %
0.02	**MAPE=4.6 %**	**MAPE=4.0 %**	**MAPE=9.1 %**	**MAPE=4.4 %**
0.01	MAPE=4.5 %	MAPE=3.9 %	MAPE=9.1 %	MAPE=4.3 %

* α = angle of the water intake, V_{res} = resultant velocity, and k = turbulent kinetic energy.

Based on the mesh sensitivity analysis, for the meshing of the solution domain, at the channel bed, a uniform wall-normal grid spacing of 0.02 meters was applied in the x and z-directions. However, the wall-normal grid spacing in the y-direction was gradually refined toward the porous region. Accordingly, a grid size of 0.005 m was employed in the first cell perpendicular to the porous zone. For all simulations, a structured rectangular mesh was used, yielding a total cell count of 0.42×10^6 within the entire computational domain.

4. Results and Discussion

The mean absolute percentage error (MAPE) is a statistical metric to determine the prediction accuracy of a model and it is calculated from the following expression:

$$MAPE\ (\%) = \frac{1}{n}\sum\left|\frac{Actual\ Value - Simulated\ Value}{Actual\ \mathrm{Value}}\right| x\ 100 \tag{6}$$

where n refers to the total number of measurement points. To this end, the mean absolute percentage error (MAPE) values between the experimental data of [13] and the CFD model results were obtained for two parameters: (i) the local resultant velocity, V_{res}, and (ii) the turbulent kinetic energy, k. Table 4 summarizes the corresponding values of the percentage errors for both Oppermann and rectangular profiles with respect to 30° and 45° angled cases. The results revealed that, for both angles, the MAPE values for the Oppermann profile are lower than the rectangular profile, especially for the turbulent kinetic energy. Considering both parameters, the best case having the lowest percentage error was found as the 30° angled Oppermann profile. However, for all cases, the MAPE values do not exceed the maximum acceptable limit of around 10%. As reported in [11] and [12], the so-called range is consistent with the literature research. Thus, it can be concluded that the Darcy-Forchheimer model applied as a porous media approach might provide a strong prediction accuracy of flow fields and turbulent quantities for water intakes. The CFD results further indicated that, for all simulations, modeling the water intakes as a porous region substantially decreased the total number of cells, which in turn resulted in a significant reduction in both computational cost and time.

Table 4. Mean absolute percentage error (MAPE) values between the experimental data of [13] and Darcy-Forchheimer model results. For validation, 60 and 90 data points were used for rectangular and Oppermann profiles, respectively. Turbulence model=LES.

Parameter	Oppermann Profile (b=10 mm)		Rectangular Profile (b=20 mm)	
	$\alpha = 30°$	$\alpha = 45°$	$\alpha = 30°$	$\alpha = 45°$
V_{res} (m/s)	4.6 %	9.1 %	5.6 %	10.7 %
k (m^2/s^2)	4.0 %	4.4 %	8.7 %	8.5 %

* α = angle of the water intake, b = clear bar spacing, V_{res} = resultant velocity, and k = turbulent kinetic energy.

Figure 3 and Figure 4 compare the experimental and numerical turbulent kinetic energy (TKE) values on the x-z vertical plane for the downstream of the Oppermann and rectangular profiles, respectively, where both figures are plotted for α= 30°. Here, the experimental contour plots (Figures 3a and 4a) show the results of the original bar geometries, whereas the CFD contour plots (Figures 3b and 4b) represent the results of the Darcy-Forchheimer porous media approach. It can be inferred that, for both Oppermann and rectangular profiles, the spatial distribution patterns of TKE that were obtained numerically are quite similar to the experimental patterns. This result indicates a well-established CFD model where the water intake is modeled as a porous medium, yielding a strong agreement between the experimental and CFD results. Moreover, this result might also be attributed to the fact that the Darcy-Forchheimer model is coupled with the LES in this present study. Compared to the Reynolds-Averaged Navier-Stokes (RANS) models, the LES turbulence model was reported to capture the vortical structures at a higher resolution within a 3D flow domain [18, 19, 20], pointing out the strong turbulence prediction accuracy of the Darcy-Forchheimer model.

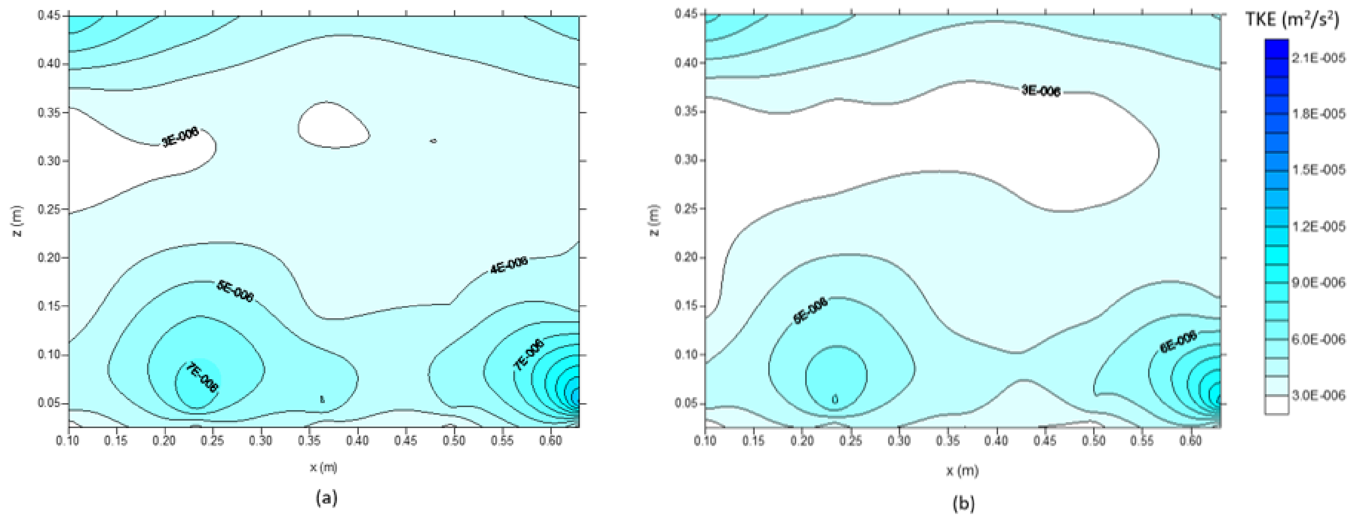

Fig. 3: Downstream TKE contours on the x-z vertical plane for the Oppermann screen: (a) experimental data of Koczula (2016) and (b) CFD model data with Darcy-Forchheimer porous media approach. $\alpha = 30°$, b =10 mm, $U_0 = 0.5$ m/s, $Fr_1 = 0.206$.

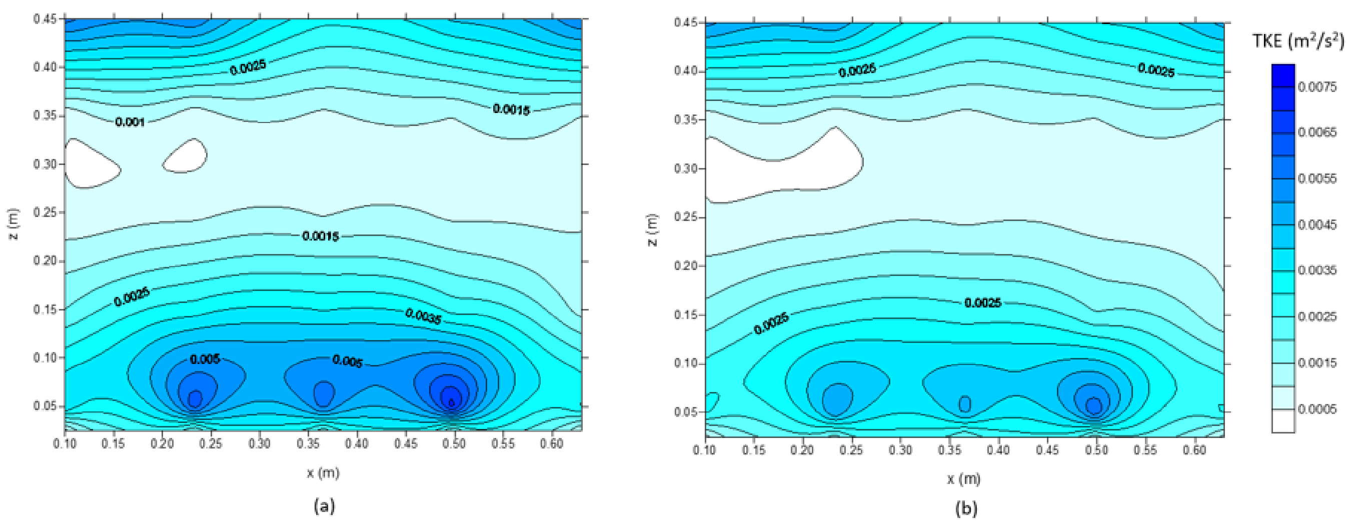

Fig. 4: Downstream TKE contours on the x-z vertical plane for the rectangular trash rack: (a) experimental data of Koczula (2016) and (b) CFD model data with Darcy-Forchheimer porous media approach. $\alpha = 30°$, b =20 mm, $U_0 = 0.5$ m/s, $Fr_1 = 0.206$.

5. Conclusion

The flow field and turbulent quantities were predicted by employing the Darcy-Forchheimer model while modeling the water intakes as a porous medium. Numerical simulations were carried out for both rectangular and Oppermann profiles under two different horizontal angles. The LES was applied for the treatment of turbulence in the CFD model, and the corresponding numerical results were compared with the experimental data, revealing an acceptable level of prediction errors for all cases. It was concluded that the Darcy-Forchheimer porous media model coupled with LES can be applicable in modeling the water intakes with high prediction accuracies. Finally, this porous media model can be implemented with coarser mesh sizes, leading to a notable reduction in the computational cost and time.

Acknowledgements

All simulations performed within the scope of this paper are supported by the Hacettepe University Scientific Research Project Program (BAP) grant with the agreement number FHD-2023-20760.

References

[1] M. Kastinger, I. Albayrak, L. G. M. Silva, and R. Boes, "Passage of downstream moving fish at a bypass gate with bottom opening," in Proc. 40th IAHR World Congress, Vienna, Austria, Aug. 21–25, 2023. doi: 10.3850/978-90-833476-1-5_iahr40wc-p0082-cd.

[2] V. Stoilova, P. Andreasson, D. Aldvén, and L. Greenberg, "Novel 'dancing rods' behavioural barrier for the guidance of juvenile salmonids," in Proc. 40th IAHR World Congress, Vienna, Austria, Aug. 21–25, 2023. doi: 10.3850/978-90-833476-1-5_iahr40wc-p1481-cd.

[3] S. Kucukali, R. Hassinger, and A. Turan, "A two-dimensional numerical and experimental study on fish-friendly hydrodynamic fine screens," in Proc. 5th IAHR Europe Congress, Trento, Italy, 2018.

[4] F. Smasal, "The most economical form of fish protection," in Proc. Hydroelectric Power between Ruhr and Lahn Conf., Brilon, Germany, 2015. (in German)

[5] F. Lemkecher, L. Chatellier, D. Courret, and L. David, "Contribution of different elements of inclined trash racks to head losses modeling," Water, vol. 12, no. 4, p. 966, 2020.

[6] S. Raynal, L. Chatellier, D. Courret, M. Larinier, and L. David, "An experimental study on fish-friendly trashracks - Part 2. Angled trashracks," J. Hydraul. Res., vol. 51, no. 1, pp. 67–75, 2013.

[7] S. Raynal, L. Chatellier, D. Courret, M. Larinier, and L. David, "Streamwise bars in angled trashracks for fish protection at water intakes," J. Hydraul. Res., vol. 52, no. 3, pp. 426–431, 2014.

[8] M. Szabo-Meszaros, C. U. Navaratnam, J. Aberle, A. T. Silva, T. Forseth, O. Calles, and K. Alfredsen, "Experimental hydraulics on fish-friendly trash-racks: an ecological approach.", Ecological Engineering, 113, 11-20, 2018.

[9] C. Beck, I. Albayrak, J. Meister, and R. M. Boes, "Hydraulic performance of fish guidance structures with curved bars: part 1: head loss assessment," J. Hydraul. Res., vol. 58, no. 5, pp. 807–818, 2020.

[10] F. Lemkecher, L. Chatellier, D. Courret, and L. David, "Experimental study of fish-friendly angled bar racks with horizontal bars," J. Hydraul. Res., vol. 60, no. 1, pp. 136–147, 2021.

[11] S. Raynal, L. Chatellier, L. David, D. Courret, and M. Larinier, "Numerical simulations of fish-friendly angled trashracks at model and real scale," in Proc. 35th IAHR World Congress, Chengdu, China, 2013.

[12] C. Leuch, C. Beck, I. Albayrak, D. F. Vetsch, and R. Boes, "Analysis and optimization of hydraulic characteristics at fish guidance structures using CFD," in Proc. 39th IAHR World Congress, Granada, Spain, Jun. 19–24, 2022, pp. 3721–3728.

[13] S. Koczula, "Hydraulic investigation of the effects of the angled flow on the fish screen," Bachelor thesis, Univ. of Kassel, Germany, 2016. (in German)

[14] FLOW-3D, User Manual; Excellence in Flow Modelling Software, ver. 11.2, Flow Science, Inc., Santa Fe, NM, 2016.

[15] S. B. Pope, Turbulent Flows, Cambridge: Cambridge Univ. Press, 2000.

[16] W. Rodi, G. Constantinescu, and T. Stoesser, Large-Eddy Simulation in Hydraulics, IAHR Monograph, CRC Press, The Netherlands, 2013.

[17] C. Ozbey and S. Kucukali, "A numerical investigation of hydrodynamics of fish-friendly fine screens," in Proc. 40th IAHR World Congress, Vienna, Austria, Aug. 21–25, 2023, pp. 1935–1944. doi: 10.3850/978-90-833476-1-5_iahr40wc-p0241-cd.

[18] F. Sotiropoulos, "Hydraulic engineering in the era of extreme-scale computing and data-driven modeling," in Proc. 7th IAHR Europe Congress, Athens, Greece, Sep. 7–9, 2022, p. 19.

[19] S. Kang, "Large-eddy simulation study of turbulent flow around a rectangular spur dike," in Proc. River Flow Conf., Lyon, France, 2018.

[20] A. L. Quaresma, F. Romao, P. Branco, M. T. Ferreira, and A. N. Pinheiro, "Multi slot versus single slot pool-type fishways: A modelling approach to compare hydrodynamics," Ecol. Eng., vol. 122, pp. 197–206, 2018.